Coherent pair production by photons in the 20-170 GeV energy range incident on crystals and birefringence

A. Apyan,[1,*] R.O. Avakian,[1] B. Badelek,[2] S. Ballestrero,[3] C. Biino,[4,5] I. Birol,[6] P. Cenci,[7] S.H. Connell,[8] S. Eichblatt,[6] T. Fonseca,[6] A. Freund,[9] B. Gorini,[5] R. Groess,[8] K. Ispirian,[1] T.J. Ketel,[10] Yu.V. Kononets,[11] A. Lopez,[12] A. Mangiarotti,[3] B. van Rens,[10] J.P.F. Sellschop,[8,†] M. Shieh,[6] P. Sona,[3] V. Strakhovenko,[13] E. Uggerhøj,[14,‡] U.I. Uggerhøj,[15] G. Unel,[6] M. Velasco,[5,§] Z.Z. Vilakazi,[8,¶] and O. Wessely[2]

(The NA59 Collaboration)

[1] *Yerevan Physics Institute, Yerevan, Armenia*
[2] *Uppsala University, Uppsala, Sweden*
[3] *INFN and University of Firenze, Firenze, Italy*
[4] *INFN and University of Torino, Torino, Italy*
[5] *CERN, Geneva, Switzerland*
[6] *Northwestern University, Evanston, USA*
[7] *INFN, Perugia, Italy*
[8] *Schonland Research Centre - University of the Witwatersrand, Johannesburg, South Africa*
[9] *ESRF, Grenoble, France*
[10] *NIKHEF, Amsterdam, The Netherlands*
[11] *Kurchatov Institute, Moscow, Russia*
[12] *University of Santiago de Compostela, Santiago de Compostela, Spain*
[13] *Institute of Nuclear Physics, Novosibirsk, Russia*
[14] *Institute for Storage Ring Facilities, University of Aarhus, Denmark*
[15] *University of Aarhus, Aarhus, Denmark*

(Dated: November 2, 2013)

The cross section for coherent pair production by linearly polarised photons in the 20-170 GeV energy range was measured for photon aligned incidence on ultra-high quality diamond and germanium crystals. The theoretical description of coherent bremsstrahlung and coherent pair production phenomena is an area of active theoretical debate and development. However, under our experimental conditions, the theory predicted the combined cross section and polarisation experimental observables very well indeed. In macroscopic terms, our experiment measured a birefringence effect in pair production in a crystal. This study of this effect also constituted a measurement of the energy dependent linear polarisation of photons produced by coherent bremsstrahlung in aligned crystals. New technologies for manipulating high energy photon beams can be realised based on an improved understanding of QED phenomena at these energies. In particular, this experiment demonstrates an efficient new polarimetry technique. The pair production measurements were done using two independent methods simultaneously. The more complex method using a magnet spectrometer showed that the simpler method using a multiplicity detector was also viable.

PACS numbers: 34.80, 32.80, 78.70.-g, 95.75.Hi, 13.88.+e
Keywords: Single Crystal, Coherent Bremsstrahlung, Polarised Photons, Polarimetry

I. INTRODUCTION

This work focuses on polarisation phenomena in coherent bremsstrahlung (CB) and coherent pair production (CPP) at high energies in oriented single crystals. The CB and CPP theories are constructed in the framework of the first Born approximation in the crystal potential [1, 2]. These theories are well established and experimentally investigated for relatively low energy (up to a few tens of GeV) electrons and photons. The theoretical description of those phenomena in oriented single crystals becomes very interesting at higher energies. The processes have an strong angular and energy dependences and the validity conditions of the Born approximation no longer hold at very high energies and small incidence angles with respect to the crystal axes and planes. The onset of this problem for the description of radiation emission and pair production has the characteristic angle $\theta_v = U_0/m$ [3], where U_0 is the plane potential well depth, m is the electron rest mass and $\hbar = c = 1$. The radiation and pair production processes can be described by the CB and CPP theory for the incidence angles with respect to the crystal axes/planes $\theta \gg \theta_v$. For angles $\theta \sim \theta_v$ and $\theta < \theta_v$ a different approach, known as the quasi classical description is used. In this approach the general theory of radiation and pair production are developed based on the quasi classical operator method [3, 4].

*Now at: Northwestern University, Evanston, USA
†Deceased
‡Co-Spokeperson
§Co-Spokeperson; Now at: Northwestern University, Evanston, USA
¶Now at: University of Cape Town, Cape Town, South Africa

Historically, the pair conversion in a single crystals was proposed, and later successfully used in the 1960s as a method to measure linear polarisation for photons in the 1-6 GeV range [5], It was predicted theoretically and later verified experimentally [6] that the pair production cross section and the sensitivity to photon polarisation increases with increasing energy. Therefore, at sufficiently high photon energies, a new polarisation technique based on this effect can be constructed, which will become competitive to other techniques, such as pair production in amorphous media and photo nuclear methods.

In the experiment, the cross section for coherent pair production by polarised photons incident on aligned germanium and diamond crystals was measured, for different carefully selected crystallographic orientations. This process can be effectively viewed as due to the imaginary part of the refractive index, as it leads to an extinction of the photon beam. It constitutes a birefringence phenomenon, as the imaginary part of the refractive index will differ as a function of the angle between the plane of polarisation of the photon beam and a specific crystallographic orientation of the "analyser" crystal. A polarimeter was constructed by measuring the energy dependent asymmetry with respect to the two most distinct orientations of the analyser crystal with respect to pair production.

The comparison to the data could validate the calculation of the energy dependence of the cross section and the polarisation of photons produced by coherent bremsstrahlung as well as the calculation of coherent pair production for polarised photons incident on crystals of different crystallographic orientations.

This paper starts with a brief discussion of the mechanism behind the creation of the polarised photon beam and its Monte Carlo (MC) simulation. After presenting the motivations and the theory behind the method used, the NA59 setup and analysis are discussed. The linear photon polarisation measurement results using various analyser crystals are followed by a comment on the possible applications of polarimetry with aligned crystals.

II. PRODUCTION OF LINEARLY POLARISED PHOTONS

In the production of photon beams, single crystals can play an important role by exploiting coherence and strong field effects that arise for oriented incidence in the interaction of radiation and matter in crystalline materials [7]. The Coherent Bremsstrahlung (CB) method is a well established one for obtaining linearly polarised photons starting from unpolarised electrons [1, 2]. An electron impinging on a crystal will interact coherently with the electric fields of the atoms in aligned crystal planes. If the Laue condition is satisfied, the bremsstrahlung photons will be emitted at specific energies corresponding to the selected vectors of the reciprocal lattice. The maximum polarisation and the maximum peak intensity occur at the same photon energy, and this energy can be selected by choosing the orientation of the lattice planes with respect to the incoming electron beam. This property has been used previously to achieve photon beams with up to 70% linear polarization starting from 6 GeV electrons [8], and up to 60% linear polarisation starting from 80 GeV electrons [9].

The relative merits of different single crystals as CB radiators have been investigated in the past [10]. The silicon crystal stands out as a good choice due to its availability, ease of growth, and low mosaic spread. The NA59 collaboration chose to use a 1.5 cm thick Si crystal to achieve a relatively low photon multiplicity and reasonable photon emission rate as seen in Fig. 1. For an 178 GeV electron beam making an angle of 5 mrad to the <001> crystallographic axis and about 70 μrad from the (110) plane, the resulting photon beam polarisation spectrum was predicted to yield maximum polarisation of about 55% in the vicinity of 70 GeV.

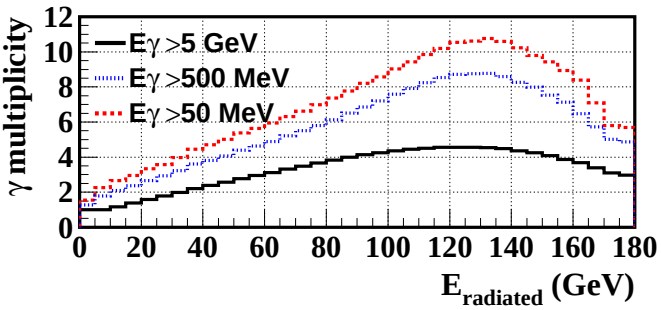

FIG. 1: MC prediction for photon multiplicity vs total radiated energy using different photon energy cut-off values.

For this choice of crystal orientation the incidence angles of electrons and photons to the crystal plane become comparable with the radiation and pair production characteristic angle θ_v. In case of the (110) plane of the silicon crystal, we find θ_v=42 μrad. In fact part of incident electron beam penetrates the crystal with angles both less and greater than θ_v, because of the angular divergence of the electron beam. In the theoretical simulations presented here, a Monte Carlo approach was used to model the divergence of the electron and photon beams, and the relevant theories (CB and CPP or the quasi classical theory) are selected as appropriate for accurate and fast calculation.

It will be shown later that this approach has lead to a very good agreement between the theoretical predications and the data.

III. CRYSTAL POLARIMETRY TECHNIQUE

In this work, the photon polarisation is always expressed using the Stoke's parametrisation with the Landau convention, where the total elliptical polarisation is decomposed into two independent linear components and

a circular component. In mathematical terms, one writes:

$$P_{\rm linear} = \sqrt{\eta_1^2 + \eta_3^2}, \quad P_{\rm circular} = \sqrt{\eta_2^2}, \quad P_{\rm total} = \sqrt{P_{\rm linear}^2 + P_{\rm circular}^2} \quad . \tag{1}$$

The radiator angular settings were chosen to have the total linear polarisation from CB radiation purely along η_3. The NA59 collaboration thus made two distinct measurements, one to show that the η_1 component of the polarisation was consistent with zero and another to find the expected η_3 component of polarisation as shown in Fig. 2.

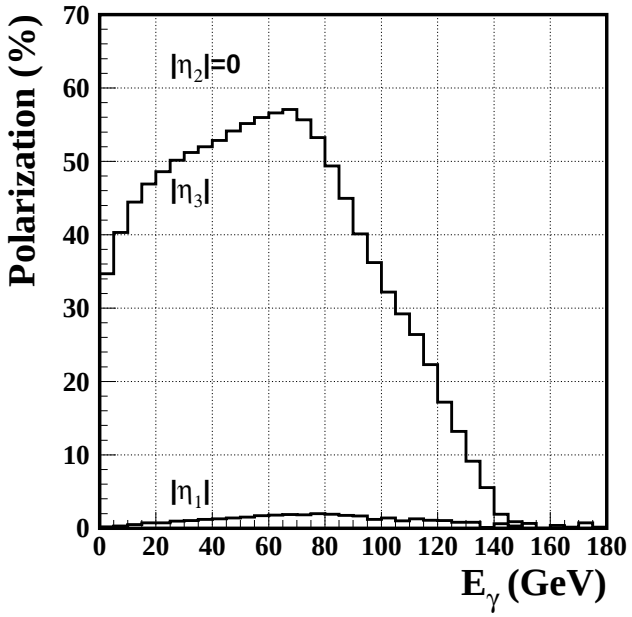

FIG. 2: Expected Polarisation for NA59 photon beam.

The MC calculations used to obtain this prediction took into account the divergence of the electron beam (48 μrad horizontally and 33 μrad vertically) and the 1% uncertainty in its 178 GeV energy. To optimise the processing time of the MC simulation, minimum energy cuts of 5 GeV for the electrons and 500 MeV for the photons were applied. We were, therefore, able to predict both the total radiated energy spectrum and the energy spectrum of individual photons, as shown in Fig. 1.

The polarisation dependence of the pair production cross section and the birefringent properties of crystals are key elements of the photon polarisation measurement. The imaginary parts of the refraction indices are related to the pair production cross section. This cross section is sensitive to the relative angle between a crystal plane of a specific symmetry and the plane of linear polarisation of the incident photon. In essence, the two orthogonal

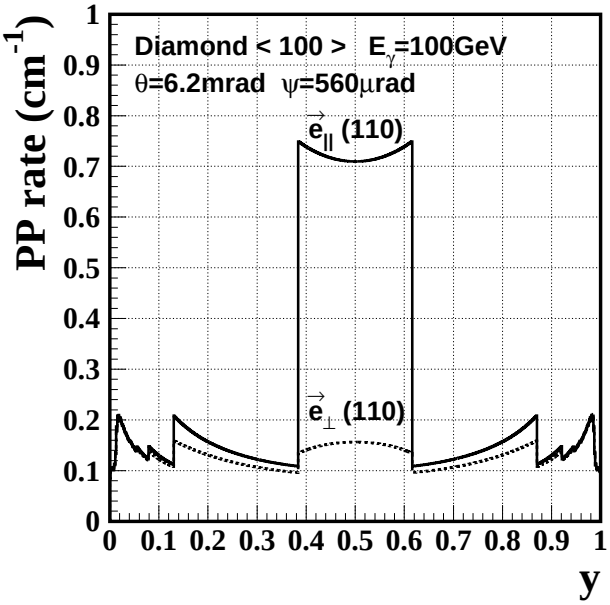

FIG. 3: Pair production rate vs the pair asymmetry, y, as defined in the text.

directions where these two planes are either parallel or perpendicular to each other yield the greatest difference in pair production cross section. We therefore studied the pairs created in a second aligned crystal, called the *analyser* crystal. In this study, the experimentally relevant quantity is the asymmetry, A, between the pair production cross sections, σ, of parallel and perpendicular polarised photons, where the polarisation direction is measured with respect to the (110) crystallographic plane of the analyser crystal. This asymmetry is related to the linear photon polarisation, $P_{\rm l}$, through the equation

$$A \equiv \frac{\sigma(\gamma_\perp \to e^+e^-) - \sigma(\gamma_\parallel \to e^+e^-)}{\sigma(\gamma_\perp \to e^+e^-) + \sigma(\gamma_\parallel \to e^+e^-)} = R \times P_{\rm l}. \tag{2}$$

Here R is the so called "analysing power" of the second crystal. The analysing power is in fact the asymmetry expected for the 100% linearly polarised photon beam. It will be seen that for the conditions of this experiment, and using the theory described, this quantity can be reliably computed using Monte Carlo simulations. In this polarimetry method, the crystal with the highest possible analysing power is preferred in order to achieve a fast

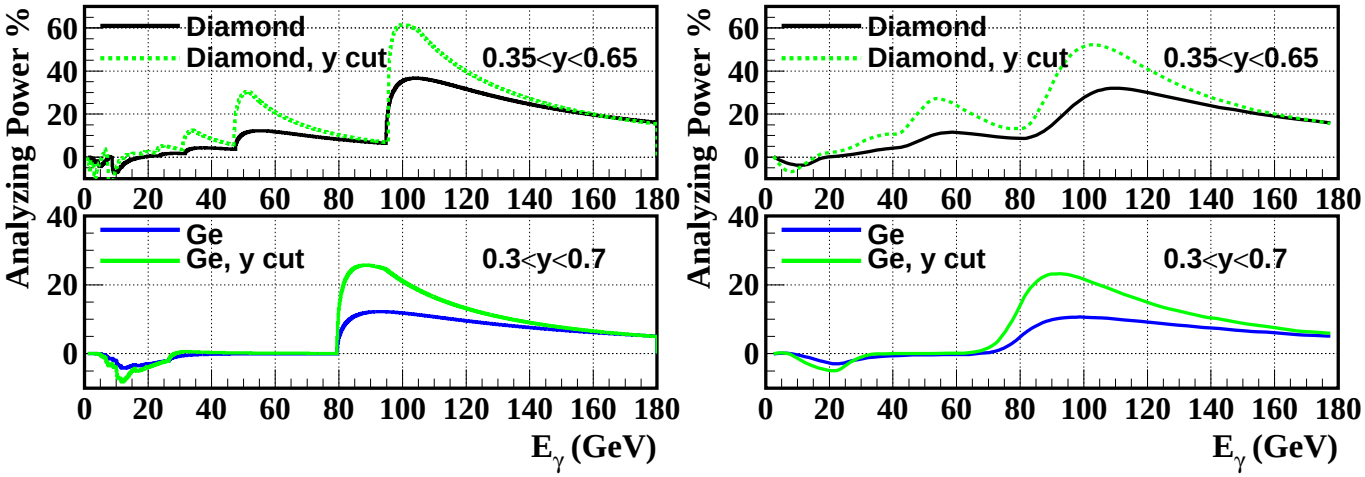

FIG. 4: Analysing power of different single crystals, for an ideal e^- beam without any angular divergences (left) and for NA59 e^- beam conditions (right).

determination of the photon polarisation.

If one defines the ratio of the energy of one member of the pairs, E^-, to the energy of the incoming photon, E_γ, as

$$y \equiv E^-/E_\gamma \quad , \tag{3}$$

then one may calculate the dependence of the pair production rate on this ratio, y, as shown in Fig. 3. By comparing the rates for the photon polarisation parallel (solid line) and perpendicular (dashed line) to the crystallographic plane, we observe that the largest difference arises for $0.4 \leq y \leq 0.6$. Therefore the pair production asymmetry may be maximised by selecting the subset of events where the e^+e^- pairs have similar energies. This method of choosing the pairs to enhance the analysing power is called the "quasi-symmetrical pair selection method" [11]. As a result of such a cut, although the total number of events decreases, the relative statistical error diminishes since it is inversely correlated with the measured asymmetry. If the efficiencies of the pair events and beam intensity normalisation events are assumed to be the same, then the cross section measurement in equation (2) reduces to counting these events separately. Denoting the number of pairs produced in perpendicular and parallel cases by p_1 and p_2, and the number of the normalisation events in each case by n_1 and n_2, respectively, the measured asymmetry can be written as:

$$A = \frac{p_1/n_1 - p_2/n_2}{p_1/n_1 + p_2/n_2}, \tag{4}$$

where p and n are acquired simultaneously and therefore correlated.

A. Analyser Crystal Options

The first analyser crystal used in the NA59 experiment was a germanium (Ge) single crystal disk with a diameter of 3 cm and a thickness of 1.0 mm. The selected orientation with respect to the incident photon beam represented a polar angle of 3.0 mrad measured from the <110> axis and an azimuthal angle corresponding to incidence exactly on the (110) plane. This configuration gave an analysing power peaking at 90 GeV, as can be seen in Fig. 4. From the same figure one can also see that the quasi-symmetrical pair selection method delivers almost twice the analysing power. The same single Ge crystal had also been used in the a previous experiment, entitled NA43. The pair production properties of this thickness of germanium crystal are therefore well known [12].

The second analyser of the NA59 experiment was a multi-tile synthetic diamond crystal target with an incident photon beam orientation with respect to the crystal of 6.2 mrad to the <001> axis and 560 μrad from the (110) plane.

The major advantage of using diamond in the analyser role are its high pair yield, high analysing power (see Fig. 4) and radiation hardness. The photon beam dimensions of NA59 implied that one would need a diamond with an area of about 20mm×20mm. A crystal thickness of 4 mm was a fair compromise between requirements of the Figure of Merit for a diamond analyser and the costs of the material. These requirements were realised by developing a composite target comprising of four synthetic diamonds of dimensions 8×8×4 mm^3 arranged in a square lattice as seen in Fig. 5. Selected areas of synthetic diamonds grown under conditions of high pressure and temperature using the "reconstitution" technique [13] and other proprietary procedures exhibit crystal structures superior to high quality natural samples. A long term program of studying large synthetic single

diamond crystals using X-ray diffraction rocking curve widths, X-ray topography [14, 15], cathodo-luminescence and indeed, experiments with coherent bremsstrahlung and pair production in experiment NA43 on a range of diamonds informed this procedure.

The four diamonds used in the composite analyser target were therefore extracted from chosen regions of selected synthetic material yielding regular tiles with optical surface finishes. The tiles had been polished with faces corresponding to cubic directions with an accuracy of about 0.2 degrees using Laue back-reflection photographs. This pre-alignment fell short of the requirements of the experiment. Each diamond tile should be mutually aligned with its neighbours so that the <001> axes normal to the tile (approximately the beam direction) corresponded within 5 μrad. In addition, the mutual azimuthal alignment of the crystallographic axes in the plane of the tile surfaces should be within 200 μrad.

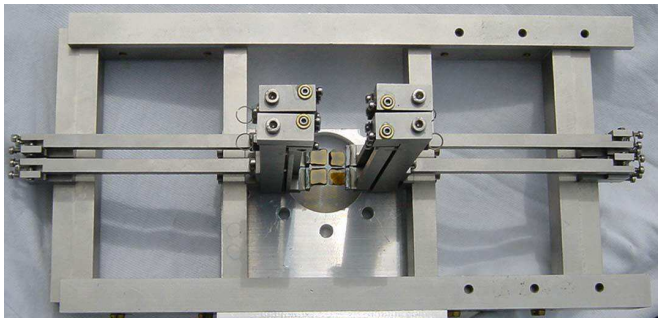

FIG. 5: The diamond analyser target consists of synthetic diamond tiles and the aluminium holder frame.

Accordingly, a mechanical system that featured three rotational degrees of freedom for each diamond tile was designed. This rotation was effected by mounting the diamond tiles on lever arms attached to a rigid frame using spring loaded flexure hinges which could be actuated by very fine threaded screws with significant mechanical advantage. Since the outer dimensions of the whole four-crystal system were limited to 300 x 150 mm we had to constrain the lengths of the lever arms to about 100 mm. The dynamic range in angle space of the lever arms was necessarily limited, requiring the diamond tiles to be pre-aligned in the adhesion mounting process. This was achieved using a goniometer mounted vacuum tweezer to offer the tile to the lever arm during fixing, under conditions of monitoring the crystallographic orientation using an X-ray system. The adhesive used was dental cement and the inter tile separation was 1 mm. The final accurate mutual alignment was performed on a precise X-ray diffractometer at CNRS, Grenoble/France using a well-collimated pencil beam. The whole alignment system shown in Fig. 5 was mounted on a high precision XY-translation table allowing each of the four crystals to be illuminated with the pencil X-ray beam in turn. The slopes of the Bragg peak at half maximum were used rather than the peak centre, as greater sensitivity could be achieved in this way. This procedure was repeated several times for all crystals to make sure that any cross-correlations between the angular rotations were eliminated. Ultimately, all lever arms were locked in position with dental cement to avoid any loss of the adjustment by vibrations during transport from Grenoble to CERN.

This last procedure corresponded to the mutual alignment between the elements of the composite target. The procedure was considered effective and can form the basis of future aligned composite target systems.

An additional fine alignment is necessary in the orientation of radiator crystal (Coherent Bremsstrahlung) and the analyser crystal (Asymmetry in Pair Production for two orthogonal Analyser crystal orientations) with the ideal particle in the beam envelope.

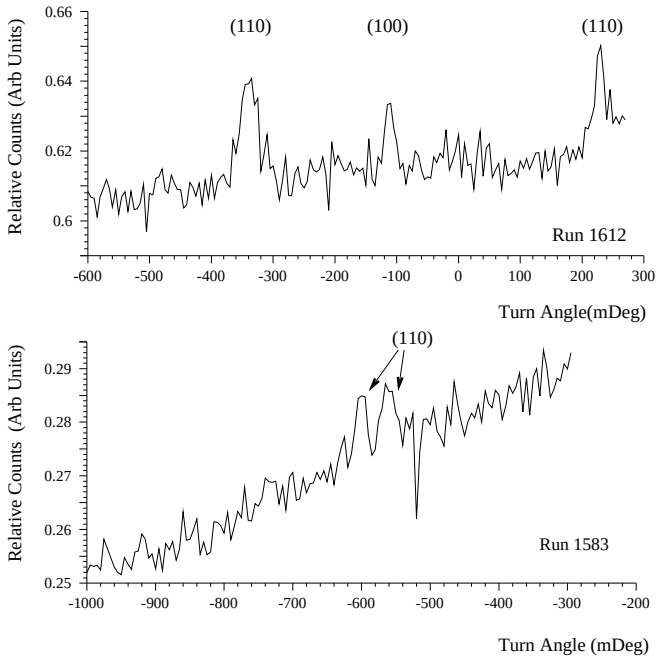

FIG. 6: TOP: Scanning across the incident angle phase space between the beam and the crystal reveals coherent enhancements of the pair-production cross-section due to planar effects, as the planes are traversed in the scan. Stereograms generated from many orthogonal scans in the region around the axis allows the identification of the crystallographic planes. BOTTOM: The mapping of the crystallographic planes revealed a misaligned tile. The misaligned tile was identified in the offline analysis.

Once beam was available, the fine alignment was performed (and indeed regularly controlled during the experiment). A narrow electron beam was directed onto the crystal, and data was collected using the minimum bias trigger. A scan of the incident angular phase space between the beam and the crystal was performed by programming the motion of the crystal mounted in the goniometers. The crystallographic axes and planes could be identified as positions in this phase space where the coherent enhancements (or reductions) of a radiation

phenomenon in relation to the corresponded incoherent cross-section occurred. This would be observed in an appropriate detector.

The radiator crystal was therefore aligned exploiting the physics of bremsstrahlung from the electron beam as observed in the Lead Glass Calorimeter. On the other hand, the analyser crystal was aligned by observing pair-production by the photon beam generated in the radiator crystal as observed in the multiplicity counter.

Stereograms of the coherent enhancements were plotted in the incident angle phase space. This allowed the planes around the axis to be accurately identified and tracked. Usually, one would explore the region around the axis, but off the axis, and then extrapolate the position of the axis using the well understood and recognised behaviour of the surrounding planes.

During the fine alignment process for the compound diamond target (Fig. 6), it was observed that one of the tiles of the multi-crystal diamond analyser was accidentally misaligned. This lead to a "doublet" when one scanned across a plane. Analysis of the stereogram indicated that one of the diamonds was out of alignment by 2.1 degrees (Fig. 6, bottom). This effect was incorporated in the offline analysis where separate spectra for each diamond of the multi-diamond target could be achieved. The offending tile was identified and excluded from the analysis.

IV. EXPERIMENT AND ANALYSIS

A. The Setup

The experimental setup for the NA59 measurements in the year 2000 is shown in Fig. 7. A 178 GeV beam of unpolarised electrons from the CERN SPS accelerator was focused on the single crystal silicon radiator (XTAL1). The crystal was of cylindrical shape with a 2.5 cm radius and a 1.5 cm thickness, and it was aligned using a goniometer of 2 μrad precision to obtain CB radiation conditions. Upstream drift chambers (dch1up-2up) allowed tracking of the incoming beam with an angular precision of 4 μrad. The drift chambers had an active area of 15×15 cm^2 divided into six cells in both horizontal and vertical planes. A double sense wire configuration removed the directional hit ambiguity. The electron emerging from the radiator crystal was tagged by two tracking chambers (dch2up and dwc3) to allow the measurement of its multiple scattering angle inside the crystal. The dwc3 is a multi wire proportional chamber [16] with an active area of about 10×10 cm and a resolution of 200 μm. A dipole magnet (Bend8) capable of a maximum beam rigidity of 4.053 Tm and a special drift chamber (dch0) with no active horizontal cells constituted the upstream spectrometer which measured the energy of the electron, before sending it to the beam dump.

After passing a helium bag of length 9.65 m to reduce the multiple scattering and background, the remaining photon beam impinged on the analyser crystal aligned with a goniometer of 20 μrad precision. The number of charged particles coming out of the analyser crystal was counted both by a scintillator (S11) for fast triggering. The photons which did not scatter or interact and the electron positron pairs created by the interacting photons continued into a magnetic spectrometer. The dipole analysis magnet (Trim6) of spectrometer was capable of a maximum beam rigidity of 0.53 Tm. The tracking elements upstream of the magnet consisted of one drift chamber (dch1) for the Ge analyser and two drift chambers (dch05 and dch1) for the diamond analyser. There were two drift chambers (dch2,dch3) downstream of the magnet. The drift chambers measured the horizontal and vertical positions of the passing charged particles with a precision of 100 μm yielding a spectrometer resolution of $\sigma/P^2 = 0.12\%$. To measure the total radiated energy, a 12-segment array lead-glass calorimeter of 24.6 radiation lengths which had a resolution of $\sigma/E = 11.5\%/\sqrt{E}$ was used. The central segment of this lead-glass array was used to map and align the crystals with an electron beam [6]. A more detailed description of the NA59 experimental apparatus is reported elsewhere [17, 18].

Various plastic scintillators were used to calibrate the tracking chambers and to define different physics triggers. The normalisation event trigger ($norm$) consisted of the signal logic combination $S1{\cdot}S2{\cdot}\overline{S3}$ to ensure that an electron is incident on the radiator crystal. The radiation event trigger (rad) was defined as the signal logic combination $norm{\cdot}(T1.or.T2){\cdot}\overline{VT}$ indicating that the incoming electron has radiated and has been successfully taken out of the photon section of the beam line. The pair event trigger ($pair$) was constructed as the signal logic combination $rad{\cdot}S11$ to select the events for which at least one e^+e^- pair was created inside the analyser crystal.

The NA59 data acquisition system consisted of personal computers running the Linux operating system and using in-house developed software to access the VME and CAMAC readout crates containing the digitisation modules. The chamber signals were read out by VME TDC modules (Caen v767) with 1 ns resolution. The scintillator and calorimeter signals were read out with CAMAC ADC modules (LRS 2249) with 0.3 pC resolution. The raw data were then stored on DLT tapes for offline analysis.

B. Analysis

The first step in the offline analysis was the beam quality cuts, which ensured the consistency of various trigger ratios and the initial beam position and angles during data taking. Next, to facilitate comparison of the experimental results with theoretical predictions, the angular divergence of the electron beam was restricted to $\pm 3\sigma$ from its mean. Determination of the electron trajectory

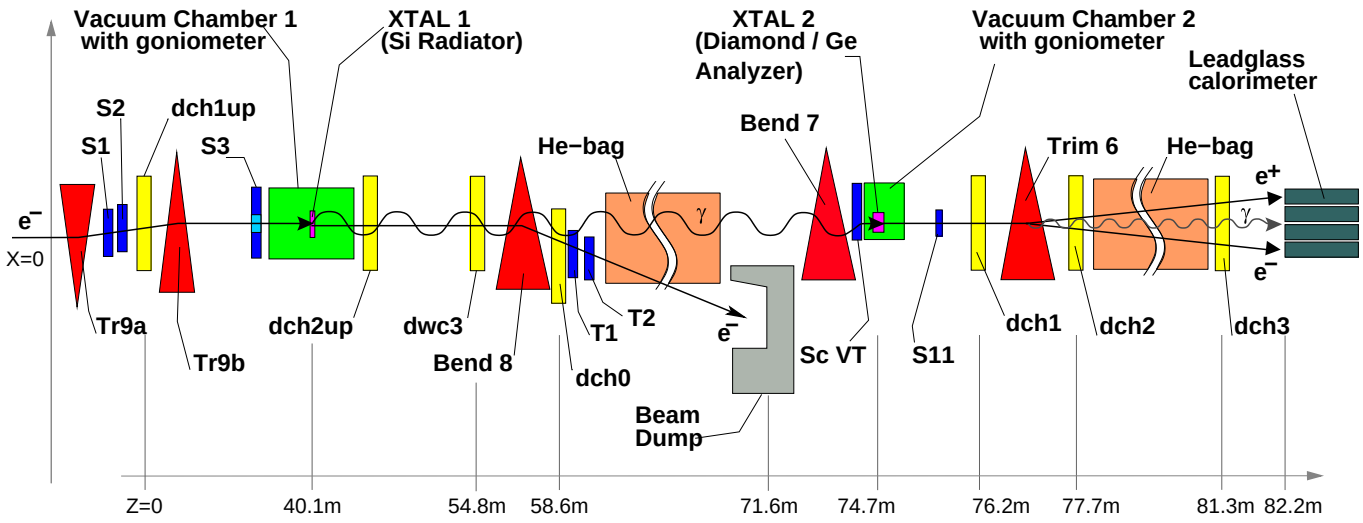

FIG. 7: The experimental setup.

and its impact point on the radiator were essential for fiducial volume requirements. The radiated photons were taken to follow the direction of the initial electron. This is accurate to $1/\gamma \approx 5\mu$rad for 100 GeV electrons. To reconstruct the single photon energy in each event, only events where a single electron positron pair was manifest in the spectrometer volume with the pair energy being the same as the photon energy were selected. This subset of pair events were further classified into families according to the number of hits on the drift chambers of the spectrometer. In our nomenclature, "122 type" events are clearly the cleanest ones with one hit in the first upstream chamber, and two in both the second and third downstream drift chambers. The resulting pair production vertex was required to be in the fiducial volume of the analyser crystal. For the case of the diamond analyser, the additional drift chamber on the downstream side ensured a better vertex reconstruction. This in turn allowed us to veto the inter-tile events as well as the ones coming from the misaligned tile. Quality assessment of the pair search program was performed by a GEANT based Monte Carlo (MC) program. This program simulated the effects of the detector geometry to understand the precision and efficiency of the reconstruction algorithm for each event family.

During the data taking, to obtain the parallel and perpendicular configurations, the angular settings of the radiator crystal (hence the direction of linear polarisation of the photon beam) were kept constant. Only the analyser crystal was rotated in a rolling motion around its symmetry axis. Therefore to measure the magnitude of the η_3 (η_1) component of the polarisation, analyser orientations separated by $\pi/2$ starting from 0 ($\pi/4$) were compared. To reduce the systematic errors, (especially in the case of the Ge crystal where the analysing power is smaller), all relevant angles on the analyser crystal were utilised for polarisation measurements, as presented in Table I. Other sources of systematic errors were the uncertainty in the crystal angles, the photon tagging and the pair reconstruction efficiencies obtained from MC studies.

TABLE I: Different material and angular settings for the analyser crystal used to measure the linear polarisation components.

analyser orientation (roll wrt radiator)	analyser type	measured polarization component
$0, \frac{\pi}{2}, \pi, \frac{3\pi}{2}$	Ge	η_3
$\frac{\pi}{4}, \frac{3\pi}{4}, \frac{5\pi}{4}, \frac{7\pi}{4}$	Ge	η_1
$0, \frac{\pi}{2}$	Diamond	η_3

C. CB Validation

The angular settings of the radiator crystal were inferred from the data. The single photon intensity spectrum presented in Fig. 8 contains two different event selections superimposed on the MC prediction. The geometrical acceptance of the spectrometer for these events has a high threshold of 30 GeV, as seen from Fig. 8.

An independent method of verifying the CB settings is looking at the total electromagnetic radiation from the radiator crystal. Fig. 9 shows the total energy radiated (EdN/dE) measured by the calorimeter for the radiator crystal aligned (bottom) and unaligned (top). In terms of the radiation intensity spectrum, an unaligned crystal is identical to an amorphous material. This radiation is called the Incoherent Bremsstrahlung (IB) and it can be approximated by the familiar Bethe-Heitler formula [19].

The increase in the CB radiation intensity spectrum is usually reported with respect to the IB spectrum. This ratio, called the "enhancement", is presented in Fig. 10 together with MC prediction for CB angle at 70 μrad. The agreement of the data with the enhancement prediction is remarkable. The offline analysis could therefore

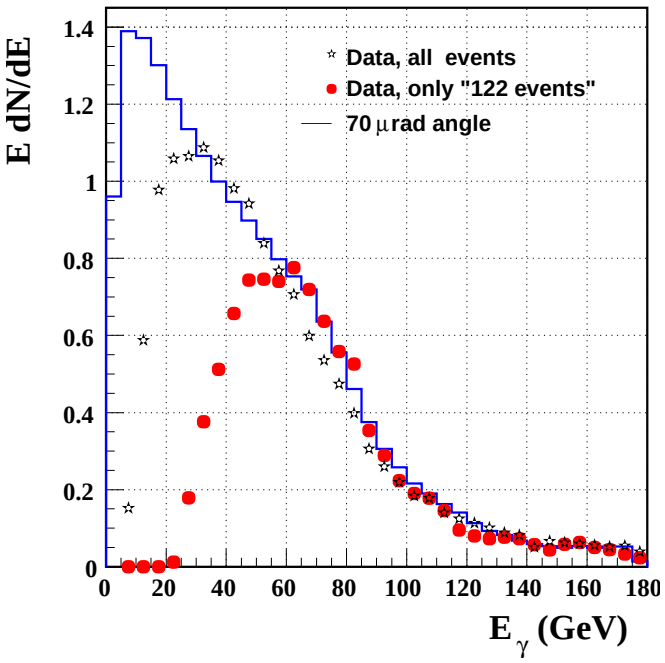

FIG. 8: MC predictions for the single photon spectrum, compared with data using all events (stars) and only '122 family' events (circles).

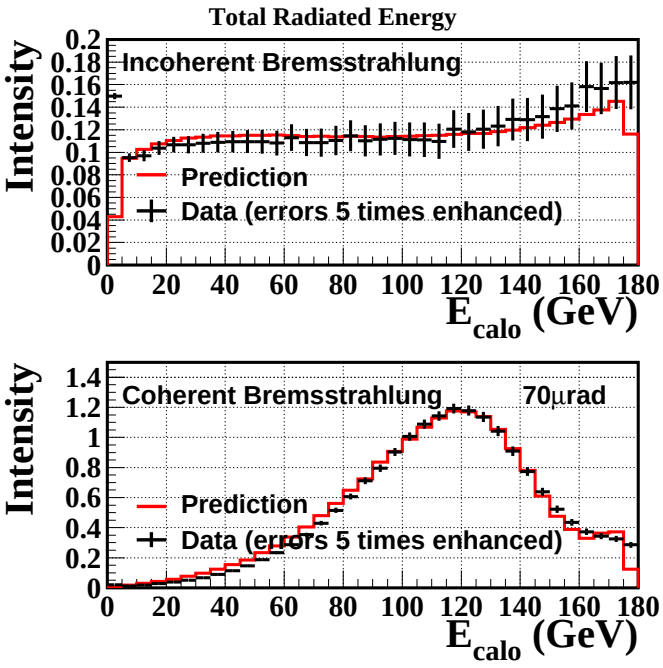

FIG. 9: Total energy radiated for Incoherent (top) and Coherent (bottom) bremsstrahlung radiation. Note the sensitivity of the cross section to small changes in the angular setting of the crystal. The statistical errors on the data are enhanced by a factor of five to increase visibility.

be used to monitor the angular settings of the radiator in time steps, to ensure the crystal angular settings did not drift during the measurement.

V. RESULTS AND CONCLUSIONS

Establishing the CB orientation allows the comparison of the predicted and measured asymmetries for both linear polarisation components: η_1 and η_3. Using all events, as well as events passing the quasi-symmetrical pairs selection criteria, we see that, as expected, the asymmetry in Fig. 11 is consistent with zero yielding a vanishingly small η_1 component of the polarization.

The measured asymmetry in the induced polarization direction (η_3) is presented in Fig. 12 without and with the y-cut using the Ge analyzer crystal. The solid line represents the MC predictions without any smearing in the spectrometer. The lower plot represents the increase in the asymmetry due to quasi-symmetrical pairs together with the statistical error associated with this increase. It thus confirms the non statistical source of the asymmetry increase in the 70-110 GeV range.

The same asymmetry as measured by the diamond analyzer is given in Fig. 13. The top and middle plots are again the asymmetry measurements as compared to the MC predictions without any smearing, and the lower plot is the increase in the asymmetry due to the y-cut. Comparing Fig. 12 and 13, we conclude that the multi-tile synthetic diamond crystal is a better choice than the Ge crystal as an analyzer, since for the same photon polarization the former yields a larger asymmetry and thus enables a more precise measurement. The diamond analyzer also allowed the measurement of the photon polarization in the 30-70 GeV range, since it has some, albeit small, analyzing power at these energies.

The theoretical predictions are based both on the calculation of the energy dependent polarisation of photons produced by coherent bremsstrahlung and the polarisation dependence of coherent pair production, also as a function of incident energy. Thus the polarisation sensitive versions of both coherent bremsstrahlung and coherent pair production are needed together in the theoretical calculation that predicts the measured asymmetry. The theoretical predictions are based both on the calculation of the energy dependent polarisation of photons produced by coherent bremsstrahlung and the polarisation dependance of coherent pair production, also as a function of incident energy. The agreement of this combined theory with the measured data is remarkable. It is clear that, for the energy range of 30-170 GeV and the incident angle phase space of this study, that the theory is sufficiently reliable and well understood to support the development of applications of crystals as polarimetry devices. The calculation of the resolving power (R in equation 2) is therefore reliable for the energy and angle regimes discussed in the introduction. The assymmetry measurements therefore correspond to a measurement of the induced polarisation fo CB for η_3 shown in Fig. 2. This has a maximum of 57% at 70 GeV. The experimen-

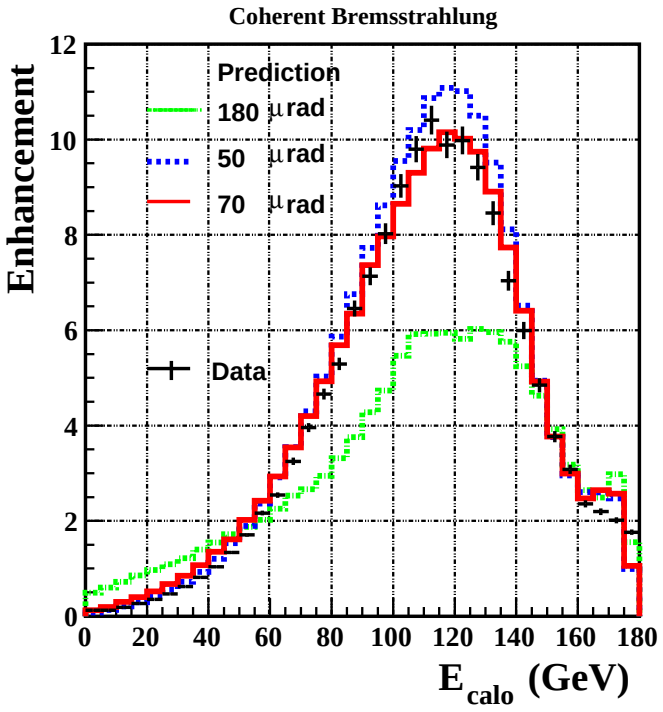

FIG. 10: Enhancement of CB radiation data compared to MC predictions.

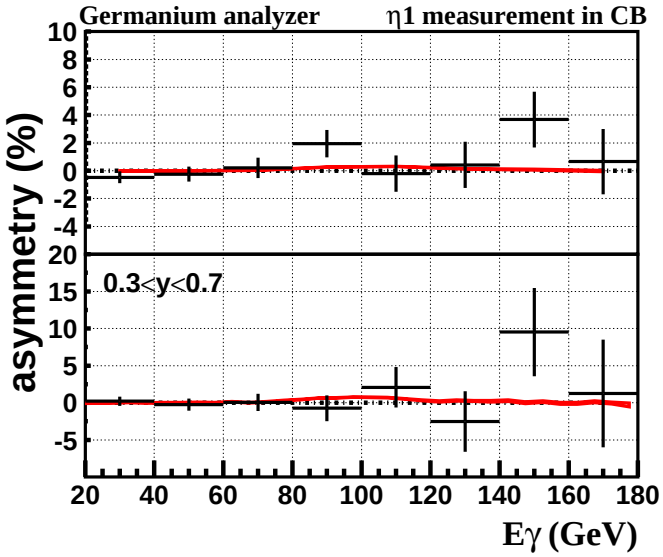

FIG. 11: Asymmetry to determined η_1 component of the photon polarization with the Ge analyzer. The data at roll angles $\pi/4{+}5\pi/4$ are compared to $3\pi/4{+}7\pi/4$ *without (TOP)* and *with (BOTTOM)* the quasi-symmetrical pair selection.

tal measured and predicted degree of linear polarization (Stokes parameter η_3) are presented in [20].

These results then show the feasibility of the use of aligned crystals as linearly polarized high energy photon beam sources. From the experimental point of view, for the creation of a photon beam with a predictable spectrum the crucial components are (i) high precision go-

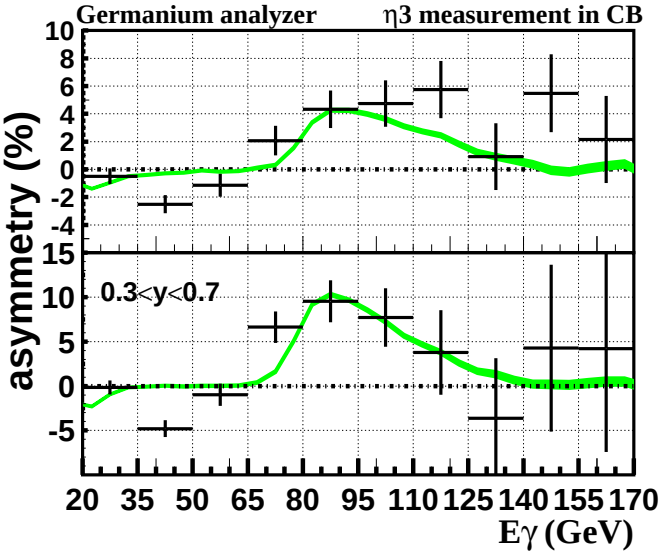

FIG. 12: Asymmetry to determine the η_3 component of the photon polarization with the Ge analyzer. Measurements *without (TOP)* and *with (BOTTOM)* the quasi-symmetrical pair selection at roll angles $0+\pi$ are compared to those at roll angles $\pi/2+3\pi/2$.

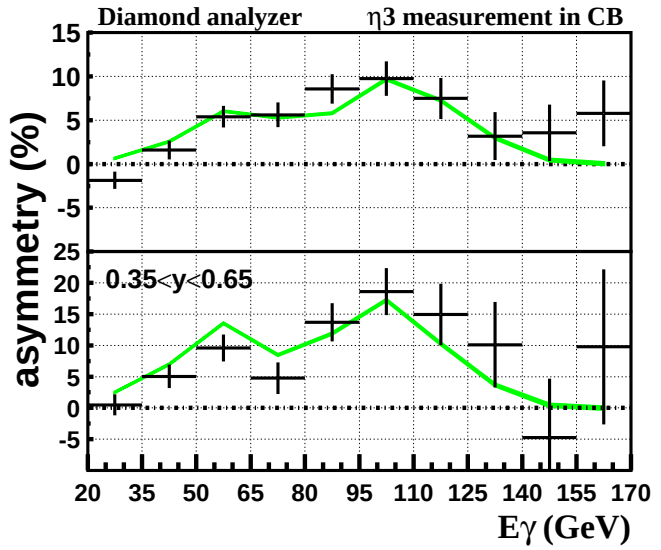

FIG. 13: Asymmetry measurements *without (TOP)* and *with (BOTTOM)* the quasi-symmetrical pair selection to determine η_3 component of the photon polarization with the *diamond* analyzer (Cf. Table I).

niometers to align the radiator crystal with respect to the electron beam and (ii) the electron beam tracking chambers to monitor the angles of incidence on the crystal surface. The predictability of the photon energy and polarization is a good asset for designing future beamlines and experiments. These results also establish the applicability of aligned crystals as polarimeters for an accurate measurement of the photon polarization at high energies. The important aspects are the analyzer ma-

terial selection and utilization of the quasi-symmetrical pairs. The use of synthetic diamond as the analyzer crystal is found to be very promising due to its availability, durability and high analyzing power.

The pair spectrometer enables the asymmetry measurement to be made for single photons in multi photon events. If the photon multiplicity is low, as it would be for laser generated beams with $E > 10\,\mathrm{GeV}$, then a simple multiplicity detector could be used to replace the more complex pair spectrometer. This is especially the case for a multiplicity detector which is energy selective. Events with higher multiplicity are known to be dominated by a single higher energy photon with the multiplicity represented by lower energy photons.

Therefore, the crystal polarimetry technique developed here should also be applicable in high energy photon beamlines as a fast monitoring tool. For example, in a future $\gamma\gamma$ or $e\gamma$ collider the quasi-online monitoring of the photon beam polarization could be achieved using this crystal polarimetry method. In the most competitive designs of such colliders [21], the photon beam after the interaction region is always taken out to a beam dump, hence the destructive nature of the crystal polarimetry technique does not constitute an impediment for its utilization. This reported polarimetry technique was successfully used in other studies of the NA59 research program [22, 23].

Acknowledgments

We dedicate this work to the memory of Friedel Sellschop. We express our gratitude to CNRS, Grenoble for the crystal alignment and Messers DeBeers Corporation for providing the high quality synthetic diamonds. We are grateful for the help and support of N. Doble, K. Elsener and H. Wahl. It is a pleasure to thank the technical staff of the participating laboratories and universities for their efforts in the construction and operation of the experiment.

This research was partially supported by the Illinois Consortium for Accelerator Research, agreement number 228-1001. UIU acknowledges support from the Danish Natural Science research council, STENO grant no J1-00-0568.

[1] M. L. Ter-Mikaelian, *High Energy Electromagnetic Processes in Condensed Media* (Wiley Interscience, New-York, 1972).
[2] G. Diambrini-Palazzi, Rev. Mod. Phys. **40**, 611 (1968).
[3] V. N. Baier, V. M. Katkov, and V. M. Strakhovenko, *Electromagnetic Processes at High Energies in Oriented Single Crystals* (World Scientific, Singapore, 1998).
[4] V. M. Strakhovenko, Phys. Rev. A **68**, 042901 (2003).
[5] G. Barbiellini, G. Bologna, G. Diambrini, and G. Murtas, Nuovo Cimento **28**, 435 (1963).
[6] R. Moore et al., Nucl. Instrum. Methods Phys. Res. B **119**, 149 (1996).
[7] K. Kirsebom et al., Nucl. Instrum. Methods Phys. Res. B **174**, 274 (2001).
[8] L. Criegee, G. Lutz, H. D. Schulz, U. Timm, and W. Zimmermann, Phys. Rev. Lett **16**, 1031 (1966).
[9] P. J. Bussey et al., Nucl. Instrum. Methods Phys. Res. **211**, 301 (1983).
[10] H. Bilokon et al., Nucl. Instrum. Methods Phys. Res. **204**, 299 (1983).
[11] A. B. Apyan et al., Nucl. Instrum. Methods Phys. Res. B **173**, 149 (2001).
[12] K. Kirsebom et al., Nucl. Instrum. Methods Phys. Res. B **135**, 143 (1998).
[13] R. C. Burns et al., J. Cryst. Growth **104**, 257 (1990).
[14] J. P. F. Sellschop et al., New Diamond and Frontier Carbon Technology **10**, 253 (2000).
[15] J. Hoszowska et al., in *Proceedings of SPIE*, edited by A. K. Freund, T. Ishikawa, and A. M. Khounsary (2001), 4501, p. 106.
[16] J. Spanggaard, CERN SL-Note-98-023 (1998).
[17] R. Groess, Master's thesis, University of Witwatersrand, South Africa (2001).
[18] O. Wessley, Master's thesis, University of Witwatersrand, South Africa (2001).
[19] W. Heitler, *The Quantum Theory of Radiation* (Dover Publications, New-York, 1984).
[20] A. Apyan et al., Nucl. Instrum. Methods Phys. Res. B (to be published).
[21] NLC Zeroth Design Report, SLAC Report 474 (1996); Tesla Conceptual Design Report, DESY 1997-048 (1997).
[22] A. Apyan et al., hep-ex/0306041.
[23] A. Apyan et al., hep-ex/0406026.